DMD Fast Forward. Published on September 7, 2007 as doi:10.1124/dmd.107.017517




# IDENTIFICATION OF HUMAN LIVER CYTOCHROME P450 ENZYMES INVOLVED IN BIOTRANSFORMATION OF VICRIVIROC, A CCR5 RECEPTOR ANTAGONIST

Anima Ghosal, Ragu Ramanathan, Yuan Yuan, Neil Hapangama, Swapan K. Chowdhury, Narendra S. Kishnani and Kevin B. Alton

Drug Metabolism and Pharmacokinetics, Schering-Plough Research Institute, Kenilworth, New Jersey.

DMD Fast Forward. Published on September 7, 2007 as DOI: 10.1124/dmd.107.017517
This article has not been copyedited and formatted. The final version may differ from this version.



**Running Title**: P450 enzymes involved in Vicriviroc metabolism

**Corresponding Author**: Anima Ghosal, Ph.D.

Drug Metabolism and Pharmacokinetics, Schering-Plough Research Institute,

2015 Galloping Hill Road, K-15-1945, Kenilworth, NJ 07033.

E-mail: anima.ghosal@spcorp.com

Number of Text pages = 25
No. of Tables = 5
No. of Figures = 9
No. of references = 24
No. of words in Abstract = 209
No. of words in Introduction = 285
No. of words in Discussion = 1002

**Abbreviations used are**: CYP, Cytochrome P450; HPLC, High performance liquid chromatography; KTZ; Ketoconazole, LC-MS, Liquid chromatography-mass spectrometry; MAb, Monoclonal antibody; NADP, Nicotine adenine dinucleotide phosphate; PBS, phosphate-buffered saline; SPE, Solid phase extraction; TRIS, Trizma-base.

DMD Fast Forward. Published on September 7, 2007 as DOI: 10.1124/dmd.107.017517
This article has not been copyedited and formatted. The final version may differ from this version.



## ABSTRACT

Vicriviroc (SCH 417690), a CCR5 receptor antagonist, is currently under investigation for the treatment of HIV infection. The objective of this study was to identify human liver cytochrome P450 enzyme(s) responsible for the metabolism of vicriviroc. Human liver microsomes (HLM) metabolized vicriviroc via N-oxidation (M2/M3), O-demethylation (M15), N,N-dealkylation (M16), N-dealkylation (M41) and oxidation to a carboxylic acid metabolite (M35b/M37a). Recombinant human CYP3A4 catalyzed the formation of all these metabolites, while CYP3A5 catalyzed the formation M2/M3 and M41. CYP2C9 only catalyzed the formation of M15. There was a high correlation between the rate of formation of M2/M3, M15 and M41, which was determined using 10 human liver microsomal samples and testosterone 6β-hydroxylation catalyzed by CYP3A4/5 ($r \geq 0.91$). Ketoconazole and azamulin (inhibitors of CYP3A4) were potent inhibitors of the formation of M2/M3, M15, M41, and M35b/M37a from human liver microsomes. A CYP3A4/5-specific monoclonal antibody (1 µg/µg protein) inhibited the formation of all metabolites from human liver microsomes by 86-100%. The results of this study suggest that formation of the major vicriviroc metabolites in human liver microsomes is primarily mediated via CYP3A4. CYP2C9 and CYP3A5 most likely play a minor role in the biotransformation of this compound. These enzymology data will provide guidance to design clinical studies to address any potential drug-drug interactions.

DMD Fast Forward. Published on September 7, 2007 as DOI: 10.1124/dmd.107.017517
This article has not been copyedited and formatted. The final version may differ from this version.



## INTRODUCTION

Cytochrome P450 (CYP) enzymes are a group of heme-containing enzymes embedded primarily in the lipid bi-layer of the endoplasmic reticulum of liver cells. CYP isoenzymes are most predominant in the liver but can also be found in the intestines, lungs and other organs. They are responsible for the oxidative, peroxidative, and reductive metabolism of a diverse group of compounds, including xenobiotics, therapeutic drugs, environmental pollutants and endobiotics such as steroids, bile acids, fatty acids, prostaglandins and leukotrienes (Nelson *et al.* 1996).

Chemokines constitute a class of cytokines that regulate migration of leucocytes to sites of infection. The CCR5 chemokine receptor is expressed on a wide range of immune cell types and binding to this receptor mediates cellular entry by the majority of HIV isolates. Blocking viral entry via this receptor reduces the viral load in patients infected with HIV, suggesting that a CCR5 antagonist could become a key component in the treatment of HIV-compromised patients (Barber, 2004). In addition, CCR5 is the main coreceptor used by macrophage (M)-tropic strains of human immunodeficiency virus type 1 (HIV-1) and HIV-2, which are responsible for viral transmission. CCR5 therefore plays an essential role in HIV pathogenesis (Blanpain et al, 2002).

Vicriviroc (SCH 417690), a CCR5 antagonist, is currently under clinical investigation for the treatment of HIV infection. The identification of the enzyme(s) responsible for the oxidative metabolism of a drug allows one to predict and/or explain interindividual differences in the effects of the drug that are due to differences in its metabolic clearance. The knowledge of the CYP450 enzymes(s) responsible for the metabolism also helps designing drug-drug interaction studies in the clinic. The

objective of this study was to identify the predominant *in vitro* biotransformation pathway(s) of vicriviroc.

## MATERIALS AND METHODS

**Chemicals.** Glucose-6-phosphate (G-6-P) dehydrogenase, monosodium D-glucose-6-phosphate, NADP, magnesium chloride, Trizma base, ammonium acetate and quinidine were purchased from Sigma-Aldrich (St. Louis, MO). Ketoconazole was purchased from Oxford Biomedical Research Inc., (Oxford, MI). HPLC grade acetonitrile, acetic acid, and methanol (Optima) from Fisher Scientific (Fair Lawn, NJ). Distilled water was prepared using a Milli-Q water purification system from Millipore (Bedford, MA). Unlabeled vicriviroc was obtained from Schering-Plough, Kenilworth, NJ. Radiolabeled vicriviroc ($^{14}$C, radiochemical purity >97%, specific activity 104 µCi/mg, Figure 1) was prepared by the Radiochemistry Group at Schering-Plough Research Institute (SPRI, Kenilworth, NJ). Pooled human liver microsomes (n=50) was purchased from XenoTech, LLC (Lenexa, KS). P450 SUPERSOMES™ and CYP3A4 monoclonal antibodies were purchased from BD-Bioscience (Woburn, MA) and HepatoScreen™ Test kit was obtained from Human Biologics (Scottsdale, AZ).

**Characterization of Metabolites:** Metabolites were characterized using a Waters Alliance HPLC system (Alliance Model 2690; Waters Corp., Milford, MA), equipped with Model 996 Photodiode Array Detector (Waters Corp.), Model 500TR flow scintillation analyzer (FSA, PerkinElmer Life & Analytical Sciences, Torrance, CA) and a 5-µm Luna Phenyl-Hexyl 250x4.6 mm column (Phenomenex, Torrance, CA). The column was maintained at room temperature for all HPLC experiments. The mobile phase consisted

of 95% 10 mM ammonium acetate with 5% acetonitrile, adjusted to pH 6.0 with acetic acid (A) and 95% acetonitrile with 5% water (B). A linear gradient was programmed as defined in the Table below:

| Time (min) | %A | %B |
|---|---|---|
| 0.00 | 90 | 10 |
| 10.00 | 70 | 30 |
| 40.00 | 30 | 70 |
| 40.10 | 10 | 90 |
| 50.00 | 10 | 90 |
| 50.10 | 90 | 10 |
| 60.00 | 90 | 10 |

A constant flow rate (1 ml/min) was maintained and the eluted drug-derived material was detected at 254 nm.

All LC-MS and LC-MS/MS experiments were performed by using a TSQ Quantum mass spectrometer (Thermo Electron Corp., San Jose, CA). The column effluent was split such that most (~80%) of the effluent was directed into the FSA and the remainder diverted to the mass spectrometer. This simultaneous detection of all drug-derived material by a MS and an FSA provided confirmation of the molecular weight and structure of all radioactive peaks in a simple experiment.

DMD Fast Forward. Published on September 7, 2007 as DOI: 10.1124/dmd.107.017517
This article has not been copyedited and formatted. The final version may differ from this version.



### LC-MS and LC-MS/MS Analysis

The mass spectrometer was nominally operated under the conditions listed in the following table with Q1 or Q3 resolution (FWHM, full width at half-maximum) set at 0.7 Th for all LC-MS and LC-MS/MS experiments.

| Parameters | Setting |
|---|---|
| Ionization Source | ESI |
| Ionization Mode | Positive |
| Spray Needle Voltage | 4.2 - 4.5 kV |
| Capillary Offset | 35 V |
| Q0 Offset | -2.0 - 2.6 V |
| Capillary Temperature | 270 - 275°C |
| Sample Flow Rate | 0.19-0.23 ml/min |
| Sheath Gas | 41 (arbitrary units) |
| Auxiliary Gas | 12 (arbitrary units) |

In LC-MS/MS experiments, ions were activated in Q2 with 25 - 30 eV collision energy while maintaining the collision gas (argon) pressure at 1.2 mtorr. Following LC-MS/FSA analysis, the area of each detected radioactive peak in the FSA was expressed as a percent of the total chromatographic radioactivity (%TCR). Percentage values for characterized metabolites, when provided are therefore estimates and not derived from a validated quantitative procedure.

### Enzyme Assays

**Incubation with Pooled Human Liver Microsomes.** To establish the optimal condition for initial velocity measurement, the linearity of vicriviroc metabolite formation was determined with respect to time (15-120 min) and microsomal P450 concentration (0.25-2 nmol/ml). Substrate concentrations of 0.1-50 µM were used to determine kinetic

parameters. All incubations (final volume 500 µl) contained microsomes, 3 mM magnesium chloride, 1 mM β-NADP, 5 mM glucose 6-phosphate, 1.5 Units/ml glucose 6-phosphate dehydrogenase and $^{14}$C-vicriviroc in 0.5 ml of 50 mM potassium phosphate buffer, pH 7.4 (Ghosal et al, 2005). The incubation mixtures were pre-warmed for 2-3 min at 37°C, reactions were initiated by the addition of substrate and then terminated with ice-cold methanol. After centrifugation (~10,000*g*) at 4°C for 10 min, each incubation supernatant was directly analyzed by HPLC. Incubations without NADPH and boiled human liver microsomes served as negative controls. Following LC analysis, metabolite concentrations were calculated based on the peak areas following FSA detection and a five point standard curve produced by linear regression. For LC-MS analysis, supernatants were concentrated under nitrogen at room temperature.

**Screening of 17 Human P450 SUPERSOMES™** *In vitro* screening of 17 human P450 SUPERSOMES™ (CYP1A1, CYP1A2, CYP2A6, CYP1B1, CYP2B6, CYP2C8, CYP2C9, CYP2C18, CYP2C19, CYP2D6, CYP2E1, CYP3A4, CYP3A5, CYP4A11, CYP4F2, CYP4F3A and CYP4F3B) were performed using a constant amount of cytochrome P450 (0.2 nmol/ml) and $^{14}$C-vicriviroc (1 and 10 µM) for 120 min. All incubations with SUPERSOMES™ were carried out as described earlier (Ghosal et al, 2005). Insect microsomes without cDNA of human P450 were used as control. For CYP2C9 and CYP2A6, incubations were performed in TRIS-buffer (supplier's recommendation). These samples were also analyzed by LC-MS. Incubations of various concentrations of vicriviroc (1-100 µM) with CYP3A4, CYP2C9 and CYP3A5 were performed to calculate kinetic parameters.

DMD Fast Forward. Published on September 7, 2007 as DOI: 10.1124/dmd.107.017517
This article has not been copyedited and formatted. The final version may differ from this version.



**Inhibition with Chemical Inhibitors and CYP3A4-Inhibitory Monoclonal Antibody**

Inhibition of vicriviroc metabolism was evaluated using both chemical inhibitors (ketoconazole, quinidine and sulfaphenazole) and inhibitory antibodies specific for CYP3A4. Human liver microsomes (0.5 nmol/ml) were preincubated with various concentrations of inhibitors/antibodies for 15 min at room temperature followed by the addition of buffer, cofactor and substrate (10 μM $^{14}$C-Vicriviroc). The final concentration of the organic solvents in the incubation system was <1%. Incubations were performed and samples were analyzed by HPLC coupled with radioactivity detector.

**Correlation Study**

The HepatoScreen™ Test Kit consisted of 10 individual human liver microsomal preparations from 10 individual donors. The ability of human liver microsomes from each donor to metabolize vicriviroc to its metabolites were correlated with the P450-specific enzyme activities for each sample from each kit. The assays were performed as described previously (under human liver microsomal incubations) with 10 μM substrate and incubated for 120 min.

**Analysis of Kinetic Data**. Untransformed enzyme kinetic data were analyzed by a nonlinear regression data analysis program (GraFit 5.0.1, Erithacus Software Limited, Staines, UK), assuming Michaelis-Menten kinetics over the substrate range studied.

DMD Fast Forward. Published on September 7, 2007 as DOI: 10.1124/dmd.107.017517
This article has not been copyedited and formatted. The final version may differ from this version.



## Results

**Optimization and Incubation with Pooled Human Liver Microsomes**.

Incubation of $^{14}$C-vicriviroc (**Figure 1**) with human liver microsomes yielded a variety of metabolites which could be separated by HPLC. When pooled human liver microsomes were incubated with 10 µM $^{14}$C-vicriviroc over a range of concentrations of cytochrome P450 (0.25- 2 nmol/ml) for various time periods (15-120 min), a P450 concentration of 0.5 nmol/ml and incubation time of 120 min were found to be optimal (**not shown**). Radiochromatographic profiles of metabolites following incubation of vicriviroc (1 and 10 µM) with human liver microsomes are presented in **Figure 2**. No metabolite formation was observed in the absence of the NADPH-generating system (not shown) or with boiled microsomes (**Figure 2**). Kinetic parameters for the production of various metabolites are shown in **Table 1**. Intrinsic clearance (Vmax/Km) data suggest that the formation of M41 (SCH 496903) and M2/M3 (SCH 643188) may be the preferred pathway for in vitro biotransformation of vicriviroc (**Table 1**). A substrate concentration of 10 µM was chosen for further experiments considering the linearity, percent of conversion and sensitivity of detection of M41.

**Screening with Human P450 SUPERSOMES™**

In vitro incubation of 1 µM vicriviroc with 17 different recombinant human P450 SUPERSOMES™ showed that CYP3A4 exhibited the most activity followed by markedly less substrate conversion with CYP3A5 and CYP2C9 (**Figures 3-4**). The major metabolite formed by CYP2C9 was M15 (SCH 495415) while CYP3A5 yielded M2/M3 (detected by LC-MS only) and M41 (**Figure 4**). CYP3A4 alone yielded the acid

metabolite M35b/M37a (SCH 727870) at 1 μM (**Figure 4**). The formation of metabolites with recombinant CYP3A4, CYP3A5 and CYP2C9 suggested possible involvement of these enzymes in the metabolism of vicriviroc. Kinetic parameters for metabolites formed following incubation of various concentrations of vicriviroc (ranging from 0.1-100 μM) with CYP3A4 and CYP3A5 SUPERSOMES™ are presented in **Table 2**. Intrinsic clearance data from CYP3A4 (Vmax/Km=25.5) and CYP3A5 (Vmax/Km=1.22) suggest that the formation of M41 is the preferred in vitro biotransformation pathway. However, incubation of vicriviroc (ranging from 0.1-50 μM) with CYP2C9 SUPERSOMES™ demonstrated atypical (biphasic) kinetics, the apparent Km and Vmax value for M15 metabolite was determined to be 672.7 μM and 1735 pmol/nmol P450/min, respectively (not shown). Kinetic parameters of other metabolites were not calculated due to lack of detection sensitivity over a range of concentrations necessary to determine Km and Vmax.

The activities of P450 SUPERSOMES™ (CYP1A1, CYP1A2, CYP2A6, CYP1B1, CYP2B6, CYP2C8, CYP2C9, CYP2C18, CYP2C19, CYP2D6, CYP3A4, and CYP3A5) obtained from BD- Bioscience (Woburn, MA) and human liver microsomes were determined in assays using fluorometric substrates as described previously (Ghosal et al, 2003). The results of the activity determination of 13 human P450 SUPERSOMES™ and human liver microsomes demonstrated that the SUPERSOMES™ and microsomes were active (not shown). The activity of CYP4A11, CYP4F2, CYP4F3A, and CYP4F3B were not determined.

**Metabolite Identification**

DMD Fast Forward. Published on September 7, 2007 as DOI: 10.1124/dmd.107.017517
This article has not been copyedited and formatted. The final version may differ from this version.



Following incubation of $^{14}$C-vicriviroc (10 μM) with CYP3A4 for 120 minutes, five major radioactive components, each representing >5% of the total chromatographic radioactivity (%TCR) and several minor to trace level drug derived components were detected. The five major components included unchanged drug (vicriviroc), the rotameric pair M2/M3, M7, M15 and M41. LC-MS spectra of unchanged drug and the four major metabolites are shown in **Figure 5**. The unchanged drug eluted at 31.1 min and exhibited a protonated ion at m/z 534. The MS/MS spectrum and the corresponding assignment of fragment ions of vicriviroc is provided in **Figure 6**. HPLC retention times, LC-MS detected m/z values and fragment ions observed in MS/MS experiments for prominent metabolites are listed in **Table 3**. The major CYP3A4 mediated metabolite, M41, had a HPLC retention time of 6.4 min and the corresponding LC-MS spectrum showed a molecular ion at m/z 332. Under the MS/MS conditions used, precursor ions at m/z 332 fragmented to give ions at m/z 101, and 135 (**Table 3**). Ions of m/z 135 and 101 respectively confirmed that 4,6-dimethyl-5-pyrimidinyl-carbonyl and methyl-1-piperazinyl moieties remained intact. Thus, M41 is most likely formed through N-dealkylation of vicriviroc. M41 was unambiguously confirmed using synthetic reference standard (SCH 496903).

Similarly, M2/M3, M7 and M15 were characterized as vicriviroc-N-oxide, vicriviroc-hydroxylamine and O-desmethyl-vicriviroc, respectively. Under the LC-conditions used, the rotameric metabolites M2/M3 eluted at 27.5/27.9 min and often were not separable. LC-MS spectrum of M2/M3 showed protonated ions at m/z 550. An increase in molecular weight of 16 Da over that of vicriviroc suggests that M2/M3 is associated with monooxidation of vicriviroc. With MS/MS conditions, precursor ions of

m/z 550 fragmented to give ions of m/z 101, 151, 203, 248, 271, 303 and 315 (**Table 3**). A 16 Da shift of the fragment ion of m/z 135 to 151 suggests that oxygenation is most likely occurring on the 4,6-dimethyl-5-pyrimidinyl-carbonyl moiety of vicriviroc. Using atmospheric pressure chemical ionization (APCI)-mass spectrometry method described previously (Ramanathan et al., 2000 and Tong et al., 2001), M2/M3 was confirmed to be an N-oxide metabolite. The structure of M2/M3 was unambiguously confirmed using a synthetic reference standard (SCH 643188).

Another significant metabolite, M15, eluted at 24.9 min and yielded protonated ions at m/z 520. The molecular weight at 519, corresponding to a decrease of 14 Da over that of vicriviroc, suggests that M15 most likely results from desmethylation of vicriviroc. Under MS/MS conditions, precursor ions at m/z 520 fragmented to give ions at m/z 101, 135, 189, 232, 289 and 301 (**Table 3**). Ions of m/z 101 and 135 respectively confirmed that methyl-1-piperazinyl and 4,6-dimethyl-5-pyrimidinyl-carbonyl-4-methylpiperidine moieties are unchanged. The absence of fragment ions at m/z 203 and 303 Th and detection of ions at m/z 189 and 289 confirmed that the ethoxy-4-trifluromethyl-phenyl-ethyl moiety has been modified by desmethylation. Furthermore, the HPLC retention time and the MS/MS spectrum of M15 matched that of a synthetic reference standard (SCH 495415).

M7, a minor *in vivo* and *in vitro* metabolite, had an HPLC retention time of 24.8 min and $[M + H]^+$ ions were observed at m/z 538. This metabolite was ~5% of the radioactivity in the CYP3A4 incubation. In incubation with human liver microsomes this metabolite was below the quantification limit and was only detected by LC-MS. An increase of 4 Da in M7 over the molecular weight of vicriviroc suggested an uncommon

metabolic modification. Precursor ions of m/z 538 fragmented to give ions at m/z 101, 139, 203, 236, 271, 303 and 315 Th (**Table 3**) under MS/MS condition. Ions at m/z 101 and 203 respectively confirmed that methyl-1-piperazinyl and ethoxy-4-trifluromethyl-phenyl-ethyl moieties are unchanged. A 4 Da shift of the fragment ion of m/z 135 to 139 suggests that an alteration is most likely occurring on the 4,6-dimethyl-5-pyrimidinyl-carbonyl moiety of vicriviroc. Modification in this region was further confirmed by a 4 Da shift of the fragment ion at m/z 232 to 236 Th. Using previously described APCI-MS and hydrogen/deuterium exchange mass spectrometry (Ramanathan et al, 2005b) and accurate mass measurement, M7 was characterized as vicriviroc-hydoxylamine. Unambiguous identification of M7 involved matching HPLC retention time and the MS/MS spectrum with that of the synthetic reference standard (SCH 727390). To our knowledge, the biotransformation of pyrimidine moiety to a pyrazyl-hydroxylamine has not been previously reported. The mechanism of this intriguing metabolic process is currently being investigated.

Other minor CYP3A4 mediated metabolites M16, M35b/M37a and M45-M47 were characterized as N, N-desalkyl-vicriviroc, vicriviroc-carboxylic acid and a series of monoxy-N-desalkyl-vicriviroc isomers. Molecular ions for M16 (SCH 496903) and M35b/M37a (SCH 727870) were observed at m/z 494 and 534 and were unambiguously confirmed using LC-MS/MS, H/D-exchange mass spectrometry and synthetic reference standards. Metabolites M45, M46 and M47 eluted between 4 and 6 minutes and exhibited $[M + H]^+$ ions at m/z 348. Although the exact position(s) of oxidation are not known, M45, M46 and M47 were characterized as monoxy metabolites of M41 (monooxy-N-desalkyl-vicriviroc) using MS/MS data.

DMD Fast Forward. Published on September 7, 2007 as DOI: 10.1124/dmd.107.017517
This article has not been copyedited and formatted. The final version may differ from this version.



Following incubation of $^{14}$C-vicriviroc with CYP2C9 and CYP3A5, on average, the unchanged drug accounted for 96% of TCR. CYP2C9 mediated metabolites with detectable radioactivity included M15 and M18/M19. M15 is a minor metabolite formed via O-demethylation of vicriviroc and M18/M19 are trace level metabolites formed by oxidation of O-desmethyl-vicriviroc. CYP3A5 mediated minor metabolites included M2/M3 and M41. Trace levels of M18/M19 were also detected in CYP3A5 incubates. The biotransformation pathway of vicriviroc is presented in **Figure 7**.

## Correlation Analysis

The formation rate of $^{14}$C-vicriviroc metabolites (M2/M3, M15, and M41) were measured in each of the 10 human liver microsomal samples provided in the HepatoScreen® Test Kit. These values were then correlated with the biochemical activity data provided by the manufacturer. Since the biochemical activity data were mediated by specific CYP enzymes, high correlation would suggest that similar enzymes were involved in the formation of metabolites from vicriviroc.

The highest correlation between the HepatoScreen® Test Kit assay data (n=10) and the formation of M2/M3, M15, M41 was noted for dextromethorphan N-demethylation ($r \geq 0.89$) which is catalyzed by CYP3A4 (**Table 4**). Correlations among M2/M3 ($r=0.91$, $p=0.0003$), M15 ($r=0.93$, $p=0.0001$), M41 ($r=0.97$, $p<0.0001$) and testosterone 6β-hydroxylation catalyzed by CYP3A4/5 were also significant (**Table 4**). A representative correlation plot of M41 is provided in **Figure 8**. There was a high correlation between the formation of metabolites and CYP2B6 activity. Interestingly, no vicriviroc metabolites were formed *in vitro* with CYP2B6 SUPERSOMES™. Nonethless,

the findings are consistent with a significant correlation between the activity of CYP2B6 SUPERSOMES™ and CYP3A4 observed by other investigators (Heyn et al, 1996). There was no significant correlation between tolbutamide methyl-hydroxylation (CYP2C9) and M15 formation. Overall, correlation analysis between the enzyme activities and metabolite formation suggested that vicriviroc is metabolized primarily by CYP3A4 in human liver microsomes.

**Inhibition Studies**

All inhibition studies were performed with pooled human liver microsomes at a drug concentration of 10 μM. Ketoconazole was shown to be a potent inhibitor of vicriviroc metabolism (all metabolites) by human liver microsomes (**Table 5**). The mean IC50 value of ketoconazole for M2/M3, M15 and M41 formation from human liver microsomes were 0.84, 1.1 and 0.79 μM, respectively (**Table 5).** Azamulin, a specific CYP3A4/5-inhibitor, inhibited M2/M3, M15 and M41 formation from human liver microsomes by 90-100% (**Table 5**) at 5 μM concentration. Neither quinidine (CYP2D6 inhibitor) at 5 μM nor sulfaphenazole (CYP2C9-specific inhibitor) at 0.5 and 3 μM had a significant effect on the metabolism of vicriviroc (**Table 5**).

Studies with CYP3A4/5-specific inhibitory monoclonal antibody showed significant inhibitory effect on the metabolism of vicriviroc (**Figure 9**). CYP3A4/5-specific inhibitory monoclonal antibody (1 μg/μg protein) inhibited the formation of M41, M2/M3, M15, M35b/M37a from human liver microsomes by 86, 83, 78 and 100%, respectively, whereas control experiments showed no inhibition.

DMD Fast Forward. Published on September 7, 2007 as DOI: 10.1124/dmd.107.017517
This article has not been copyedited and formatted. The final version may differ from this version.



## DISCUSSION

Following administration of a single oral dose of $^{14}$C-SCH 417690 (50 mg) to humans, M41, M37, M35, M15, and M2/M3 were major circulating metabolites representing at least 5% of the circulating drug derived radioactivity in 4, 8 or 24 hour plasma samples (Ramanathan et al, 2005a). The level of M35b/M37a, a carboxylic acid metabolite detected at trace level following single dose to humans, was found to increase following multiple dose administration and represented a major metabolite at steady state. All major in vivo human metabolites were identified following incubation of 10 µM $^{14}$C-SCH 417690 with human liver microsomes (**Figure 2**) with the exception of M35, which is a glucuronide conjugate of M15. M35 was not expected to be formed in this incubation with human liver microsomes without the cofactor UDPGA required to form glucuronide conjugate. The same metabolites were also detected following incubation of $^{14}$C-SCH 417690 with cDNA expressed CYP 3A4. Only M15 was detected upon incubation with CYP 2C9, and M41 and M2/M3 upon incubation with CYP 3A5 (**Figure 4**). M7, a minor metabolite in both human liver microsomal and CYP 3A4 incubations was present at trace levels in human plasma after administration of $^{14}$C-SCH 417690. Therefore, the identification of human cytochrome P450 enzymes involved in the *in vitro* metabolism of vicriviroc represented true *in vivo* human metabolites.

A multistep approach was used to identify the CYP isoform(s) responsible for vicriviroc metabolism. This "reaction phenotyping" included correlation analysis with a panel of characterized microsomal preparations, chemical and antibody inhibition, and the use of cDNA-expressed human CYP isoforms. Incubation of vicriviroc with human

liver microsomes showed that M2/M3, M15, M16, M35b/M37a and M41 were primary *in vitro* metabolites. Formation of all metabolites was mediated via CYP3A4, based on inhibition by ketoconazole, and the production of these metabolites from SUPERSOMES™ overexpressing CYP3A4. Biotransformation of vicriviroc (SCH 417690) in human liver microsomes and cDNA-expressed human P450 enzymes are shown in **Figure 7**.

*In vitro* incubation with 17 different recombinant human P450 SUPERSOMES™ showed that CYP3A4 exhibited the most activity followed by CYP2C9 and CYP3A5. The formation of metabolites with recombinant CYP2C9, CYP3A4, and CYP3A5 suggested minimal involvement of CYP2C9 and CYP3A5 in the metabolism of vicriviroc. In human liver microsomes, the apparent Km (8.92 µM) for M41 is lower than the Km values in CYP3A4 and CYP3A5 (25.6 and 51 µM). In the present study, formation of M41 from CYP3A5 is very low, only 2% converted to M41. In addition CYP3A5 plays a minor role in the metabolism of vicriviroc, therefore its Km does not reflect the Km from human liver microsomes. Differences of Km values in human liver microsomes and in recombinant systems are also reported in literature for other compounds. Yamazaki et al (1999) showed that apparent Km (28 µM) for troglitazone metabolite-3 formation in human liver microsomes is lower than Km in CYP3A4 (120 µM) but higher than the Km of other CYPs (CYP2C8, CYP2C9 and CYP2C19) involved. In case of diltiazem N-demethylation, Km in human liver microsomes is 53 µM while that in CYP3A4 is lower (16 µM) and is higher in CYP3A5 (81 µM) (Jones et al, 1999). Kumar et al (2006) also reported lower Km value for (S) warfarin and (s) flurbiprofen as 3.7 and 1.9 µM in human liver microsomes compared to CYP2C9 (13 and 21.6 µM), respectively.

Therefore, there are several evidences for the differences in Km values between human liver microsomes and recombinant CYPs in the literature. The ratio of P450 reductase to P450 or cytochtome b5 to P450 in the recombinant systems and their specific CYP content may be responsible for the apparent difference in Km values observed in human liver microsomes and recombinant CYPs.

Incubation of vicriviroc with CYP2C9 SUPERSOMES™ exhibited biphasic kinetics for the formation of M15. The profile eventually became linear with increasing substrate concentration (not shown), however, saturation was not obtained up to 100 µM. This reaction profile for production of M15 did not obey classical Michaelis-Menten kinetics. A biphasic kinetic profile is generally characterized by an initial Michaelis-Menten-like increase in velocity with increasing substrate concentration. However, the profile does not become asymptotic and eventually becomes linear with increasing substrate concentration. This behavior results in the inability to predict an apparent $V_{max}$ and $K_m$ and has previously been reported for this and other recombinant CYPs. For example the saturation of naproxen demethylation by CYP2C9 is not achieved up to 1800 µM (Korzekwa et al., 1998; Hutzler et al., 2001), and CYP3A4-mediated naphthalene metabolism to 1-naphthol continues up to 400 µM (Korzekwa et al., 1998). Examples of biphasic kinetics are becoming more prevalent with several P450 isoforms (CYP3A4, CYP2C9 etc) apparently exhibiting this type of behavior (Hutzler and Tracy, 2002). Hutzler et al, (2001) suggested that the activation of CYP2C9-mediated dapsone metabolism and its biphasic profile may be explained by a two-site binding mode. Interestingly, incubations of vicriviroc with human liver microsomes do not show

biphasic behavior for the formation of M15, as M15 is largely mediated by CYP3A4 and it also plays a minor role in the metabolism of vicriviroc.

Ketoconazole (Desai et al, 1998; Newton et al, 1995; Ghosal et al, 1996; Masimirembwa et al, 1999; Wrighton et al, 1994) and azamulin (Stresser et al, 2004) (both CYP3A4-selective inhibitor), were shown to be potent inhibitors of vicriviroc metabolism by human liver microsomes suggesting the involvement of CYP3A4 in its metabolism. Stresser et al (2004) reported that azamulin is a highly potent and selective inhibitor of CYP3A. However, sulfaphenazole (CYP2C9-selective inhibitor, Newton et al, 1995) had no significant effect on the metabolism of vicriviroc, suggesting that CYP2C9 plays a minor role in the metabolism of vicriviroc. Studies with CYP3A4/5 inhibitory antibody demonstrated that it inhibited >80% of vicriviroc metabolism in human liver microsomes. In addition, there was a significant correlation between the formation of M2/M3, M15, M41 and dextromethorphan N-demethylation or testosterone 6β-hydroxylation, known to be mediated by CYP3A4 (Newton et al, 1995; Gorski et al, 1994). These inhibition and correlation studies suggest that CYP3A4 is primarily responsible for the biotransformation of vicriviroc.

## REFERENCES

Barber CG (2004) CCR5 antagonists for the treatment of HIV. *Curr Opin Investig Drugs*.**5(8):**851-61

Blanpain C, Libert F, Vassart G, Parmentier M (2002) CCR5 and HIV infection. *Receptors Channels* **8(1):**19-31.

Crespi CL (1995) Xenobiotic-metabolizing human cells as tools for pharmacological and toxicological research. *Adv Drug Res* **26:** 179-235.

Desai PB, Duan JZ, Zhu YW and Kouzi S (1998) Human liver microsomal metabolism of paclitaxel and drug interactions. *Eur J. Drug Metab. Pharmacokinetics* **23(3)**: 417-424.

Ghosal A, Chowdhury S, Gupta S, Yuan Y, Iannucci R, Zhang H, Zbaida S, Patrick JE, and Alton KB. (2005) Identification of human liver cytochrome P450 enzymes involved in the metabolism of SCH 351125, a CCR5 antagonist. *Xenobiotica* **35(5**):405-417.

Ghosal A, Satoh H, Thomas PE, Bush E, and Moore D (1996) Inhibition and kinetics of cytochrome P450 3A activity in microsomes from rat, human and cDNA-expressed human cytochrome P450. *Drug Metab. Dispos* **24**: 940-947.

Ghosal A, Hapangama N, Yuan Y, Lu X, Horne D, Patrick JE, and Zbaida S (2003) Rapid determination of enzyme activities of recombinant human cytochromes P450, human liver microsomes, and hepatocytes. *Biopharmaceutics and Drug Dispos* **24 (9):**375-384.

Gorski JC, Jones DR, Wrighton SA, Hall SD (1994) Characterization of dextromethorphan N-demethylation by human liver microsomes. Contribution of the cytochrome P450 3A (CYP3A) subfamily. *Biochem. Pharmacol*. **48(1):** 173-82.

Heyn H, White RB and Stevens JC (1996). Catalytic role of cytochrome P4502B6 in the N-demethylation of S-mephenytoin. *Drug Metab Dispos*. **24(9):** 948-954.

Hutzler JM and Tracy TS (2002) Atypical kinetic profiles in drug metabolism reactions. *Drug Metab. Dispos*. **30(4):**355-362.

Hutzler JM, Hauer MJ and Tracy TS (2001) Dapsone activation of CYP2C9-mediated metabolism: evidence for activation of multiple substrates and a two-site model. *Drug Metab Dispos* **29:** 1029-1034.

Jones DR, Christopher GJ, Hamman MA, Mayhew BS, Rider S and Hall SD (1999) Diltiazem inhibition of cytochrome P-450 3A activity is due to metabolite intermediate complex formation. *J Pharmacol Exp Ther*. **290(3)**: 1116-1125.

Korzekwa KR, Krishnamachary N, Shou M, Ogai A, Parise RA, Rettie AE, Gonzalez FJ and Tracy TS (1998) Evaluation of atypical cytochrome P450 kinetics with two-substrate models: evidence that multiple substrates can simultaneously bind to cytochrome P450 active sites. *Biochemistry* **37:** 4137-4147.

Kumar V, Rock DA, Warren CJ, Tracy TS and Wahlstrom JL (2006) Enzyme source effects on CYP2C9 kinetics and inhibition. *Drug Metab Dispos* **34**:1903-1908.

Masimirembwa CM, Otter C, Berg M, Jonsson M, Leidvik B, Jonsson E, Johansson T, Backman A, Edlund A and Andersson TB (1999) Heterologous expression and kinetic characterization of human cytochromes P-450: Validation of a pharmaceutical tool for drug metabolism research. *Drug Metab. Dispos* **27(10):** 1117-1122.

Nelson DR, Koymans L, Kamataki T, Stegeman JJ, Feyereisen R, Waxman DJ, Waterman MR, Gotoh O, Coon MJ, Estabrook RW, Gunsalus IC & Nebert DW (1996) P450 superfamily: update on new sequences, gene mapping, accession numbers and nomenclature. *Pharmacogenetics* **6**: 1-42.

Newton DJ, Wang RW, Lu AYH (1995) Cytochrome P450 inhibitors. Evaluation of specificities in the in vitro metabolism of therapeutic agents by human liver microsomes. *Drug Metab Dispos* **23**:154-158.

Ramanathan, R.; Zhong, R.; Alvarez, N.; Kennedy, C.; Grotz, D.; Rindgen, D.; Cox, K.; Chowdhury, S.; Wirth, M.; Alton, K. (2005a) Comparative Metabolism and Excretion of a Novel CCR5 Receptor Antagonist, SCH 417690 (Vicriviroc), in Human, Monkey, and Rat. *Drug Metabolism Reviews* **37(4)**, 725-726.

Ramanathan R, Chowdhury SK, and Alton KB (2005b) "Oxidative Metabolites of Drugs and Xenobiotics: LC-MS Methods to Identify and Characterize in Biological Matrices in Drugs, Metabolites and Metabolizing Enzymes: Role of LC-MS in Identification and Quantification from Biological Matrices", edited by Swapan K. Chowdhury, Elsevier BV, The Netherlands.

Ramanathan, R.; Su, A. D.; Alvarez, N.; Blumenkrantz, N.; Chowdhury, S. K.; Alton, K. B.; Patrick J. E (2000) Liquid Chromatography/Mass Spectrometry Methods for Distinguishing N-oxides from Hydroxylated Compounds. *Anal. Chem*. ***72***: 1352-1359.

Stresser DM, , Broudy MI, Ho T, Cargill CE, Blanchard AP, Sharma R, Dandeneau AA, Goodwin JJ, Turner SD, Erve JCL, Patten CJ, Dehal SS, and Crespi. CL (2004) Highly selective inhibition of human CYP3A in vitro by azamulin and evidence that inhibtion is irreversible. *Drug Metab. Dispos*. **32 (1):**105-112.

Tong, W.; Chowdhury, S. K.; Chen, J. C.; Zhong, R.; Alton, K. B.; Patrick, J. E (2001) Fragmentation of N-oxides (Deoxygenation) in Atmospheric Pressure Ionization: Investigation of the Activation Process. *Rapid Comm. Mass Spect*., ***15:*** 2085-2090.

Wrighton SA and Ring BJ (1994) Inhibition of human CYP3A catalyzed 1′-hydroxy midazolam formation by ketoconazole, nifedipine, erythromycin, cimetidine and nizatidine. *Pharm. Res*. **11**:921-924.

Yamazaki H, Shibata A, Suzuki M, Nakajima M, Shimada N, Guengerich FP, and Yokoi, T (1999) Oxidation of troglitazone to a quinone-type metabolite catalyzed by cytochrome P-450 2C8 and P-450 3A4 in human liver microsomes. *Drug Metab Dispos* **27(11)**: 1260-1266.

## FIGURE LEGENDS

**FIG 1.** Chemical Structure of Vicriviroc. (*) denotes site of $^{14}$C-label

**FIG 2.** Radiometric Profile of Metabolites Following 120 min Incubation of $^{14}$C-vicriviroc (1 and 10 µM) with human liver microsomes (1µM, top and middle panel) and 10 µM (bottom panel) Supplemented with NADPH-generating system

**FIG 3.** Screening of P450 SUPERSOMES™ for the Formation of Metabolites from $^{14}$C-vicriviroc

**FIG 4.** Radiometric Profile of Metabolites Following 120 min Incubation of $^{14}$C-vicriviroc (10 µM) With CYP3A4 (top panel), CYP2C9 (middle panel) and CYP3A5 (bottom panel)

**FIG.5**. LC-MS Spectra of vicriviroc and its major in-vitro metabolites.

**FIG.6**. LC-MS/MS Spectrum of vicriviroc and the Proposed Fragmentation Scheme.

**FIG 7.** Biotransformation of vicriviroc (SCH 417690) in Human Liver Microsomes and cDNA-Expressed Human P450 Enzymes (Only major routes are shown)

**FIG 8.** Regression Analysis of M41 Formation Rate from $^{14}$C-vicriviroc to CYP3A4/5 Catalyzed Testosterone 6β-hydroxylase Activity in 10 Individual Human Liver Microsomes

**FIG 9.** Immunoinhibition of vicriviroc Metabolism with CYP3A4/5-Specific Inhibitory Monoclonal Antibody (MAb). Human liver microsomes were incubated with 10 µM vicriviroc and CYP3A4/5-antibody in presence of an NADPH-Generating System. (●) represents M41; (■) represents M2/M3; (▲) represents M15 and (○) represents M35b/M37a.

DMD Fast Forward. Published on September 7, 2007 as DOI: 10.1124/dmd.107.017517
This article has not been copyedited and formatted. The final version may differ from this version.



TABLE 1

*Kinetic Parameters for the Formation of Metabolites from $^{14}$C-Vicriviroc with Pooled Human Liver Microsomes*

| Kinetic Parameters[a] | M2/M3 | M15 | M16 | M41 |
|---|---|---|---|---|
| Km (μM) | 14.7±1.0[b] | 19.3±2.69 | 9.05±3.77 | 8.92±0.82 |
| Vmax (pmol/nmol P450/min) | 31.6±0.88 | 25.2±1.52 | 7.28±1.03 | 22.9±0.79 |
| Vmax/Km (μL/nmol P450/min)[c] | 2.15 | 1.30 | 0.80 | 2.56 |

a: Kinetic parameters were determined by GraFit 5.0.1 program
b: ±SE
c: Intrinsic clearance

DMD Fast Forward. Published on September 7, 2007 as DOI: 10.1124/dmd.107.017517
This article has not been copyedited and formatted. The final version may differ from this version.



TABLE 2

*Kinetic Parameters for the Formation of Metabolites from $^{14}$C-Vicriviroc with Human P450 SUPERSOMES™*

| Kinetic Parameters[a] | CYP3A4 | | CYP3A5 | |
|---|---|---|---|---|
| | M7 | M41 | M2/M3 | M41 |
| Km (μM) | 4.7±1.8[b] | 25.6±2.6 | 44.2±2.47 | 51.3±5.3 |
| Vmax (pmol/nmol P450/min) | 82.9±8.1 | 654.2±0.03 | 40.0±1.02 | 62.6±3.1 |
| Vmax/Km (μL/nmol P450/min)[c] | 17.6 | 25.5 | 0.90 | 1.22 |

a: Kinetic parameters were determined by GraFit 5.0.1 program
b: ±SE
c: Intrinsic clearance

TABLE 3

*LC-MS and LC-MS/MS Characterization of Vicriviroc Metabolites*

| Vicriviroc and Metabolites | HPLC Retention Time (min) | LC-MS Detected Molecular Ion (*m/z*) | LC-MS/MS Detected Fragment Ions (*m/z*) | Additional Structural Confirmation |
|---|---|---|---|---|
| Vicriviroc (SCH 417690) | 30.6 | 534 | 101, 135, 203, 232, 271, 303 and 315 | Reference Standard |
| M2/M3 (Vicriviroc-*N*-oxide, SCH 643188) | 27.5/27.7 | 550 | 101, 151, 203, 248, 271, 303 and 315 | Reference standard and LC-APCI-MS |
| M7 (Vicriviroc-hydroxylamine, SCH 727390) | 24.8 | 538 | 101, 139, 203, 236, 271, 303 and 315 | Reference Standard, Hydrogen-Deuterium Exchange and LC-APCI-MS |
| M15 (*O*-desmethyl-vicriviroc, SCH 495415) | 22.5 | 520 | 101, 135, 189, 232, 271, 289 and 301 | Reference Standard |
| M41 (*N*-desalkyl-vicriviroc, SCH 496903) | 6.4 | 332 | 101, 135 and 232 | Reference standard |

DMD Fast Forward. Published on September 7, 2007 as DOI: 10.1124/dmd.107.017517
This article has not been copyedited and formatted. The final version may differ from this version.



TABLE 4

*Correlation (r) Values Between Metabolite Formation Rates and P450 Enzyme Specific Activities at 10 μM Vicriviroc*

| P450 Enzyme Specific Reactions | P450 Involved[a] | M2/M3 | M15 | M41 |
|---|---|---|---|---|
| Caffeine N3-Demethylation | CYP1A2 | 0.31 | 0.43 | 0.36 |
| Coumarin 7-Hydroxylation | CYP2A6 | 0.32 | 0.29 | 0.18 |
| S-Mephenytoin N-Demethylation | CYP2B6[b] | 0.86 | 0.89 | 0.86 |
| Tolbutamide Methyl-hydroxylation | CYP2C9 | 0.09 | 0.07 | 0.18 |
| S-Mephenytoin 4'-hydroxylation | CYP2C19 | 0.48 | 0.37 | 0.39 |
| Dextromethorphan O-Demethylation | CYP2D6 | 0.29 | 0.32 | 0.14 |
| Chlorzoxazone 6-Hydroxylation | CYP2E1 | 0.23 | 0.23 | 0.61 |
| Dextromethorphan N-Demethylation | CYP3A4 | 0.90 | 0.91 | 0.89 |
| Testosterone 6β-Hydroxylation | CYP3A4/5 | 0.91[c] | 0.93[d] | 0.97[e] |
| Lauric Acid 12-Hydroxylation | CYP4A11 | 0.04 | 0.07 | 0.01 |

a: Enzyme activities are from HepatoScreen Test kit (n= 10)
b: No metabolism was observed with CYP2B6 SUPERSOMES™
c: p=0.0003; d: p=0.0001; e: p<0.0001 (calculated using GraphPad Prism 4.0)
Correlation between CYP2B6 and CYP3A4 activity is high (r = 0.98); similar observation was reported by Heyn et al (1996)

DMD Fast Forward. Published on September 7, 2007 as DOI: 10.1124/dmd.107.017517
This article has not been copyedited and formatted. The final version may differ from this version.



TABLE 5

*Effect of P450-Specific Chemical Inhibitors on Vicriviroc Metabolism with Human Liver Microsomes*

| Inhibitors | Inhibitor Conc. (μM) | Percent of control remaining ($IC_{50}$) | | | |
|---|---|---|---|---|---|
| | | M2/M3 | M15 | Acid Metabolite (M35b/M37a) | M41 |
| Ketoconazole | 0.5 | 68.1 (0.84±0.06) | 64.6 (1.1±0.06) | 64 (NP) | 56.8 (0.79±0.08) |
| | 5 | 7.15 | 8.64 | 0 | 4.4 |
| Azamulin | 0.5 | 41.3 | 41.1 | 0 | 29.6 |
| | 5 | 0 | 9.62 | 0 | 0 |
| Quinidine | 5 | 107 | 104 | NP | 108 |
| Sulfaphenazole | 0.5 | 96.7 | 103 | 99.1 | 101 |
| | 3 | 94.2 | 100 | 94.5 | 96.4 |

NP = Not performed

Values in parenthesis = $IC_{50}$

Activity remaining is calculated as % of vehicle control.

DMD Fast Forward. Published on September 7, 2007 as DOI: 10.1124/dmd.107.017517
This article has not been copyedited and formatted. The final version may differ from this version.

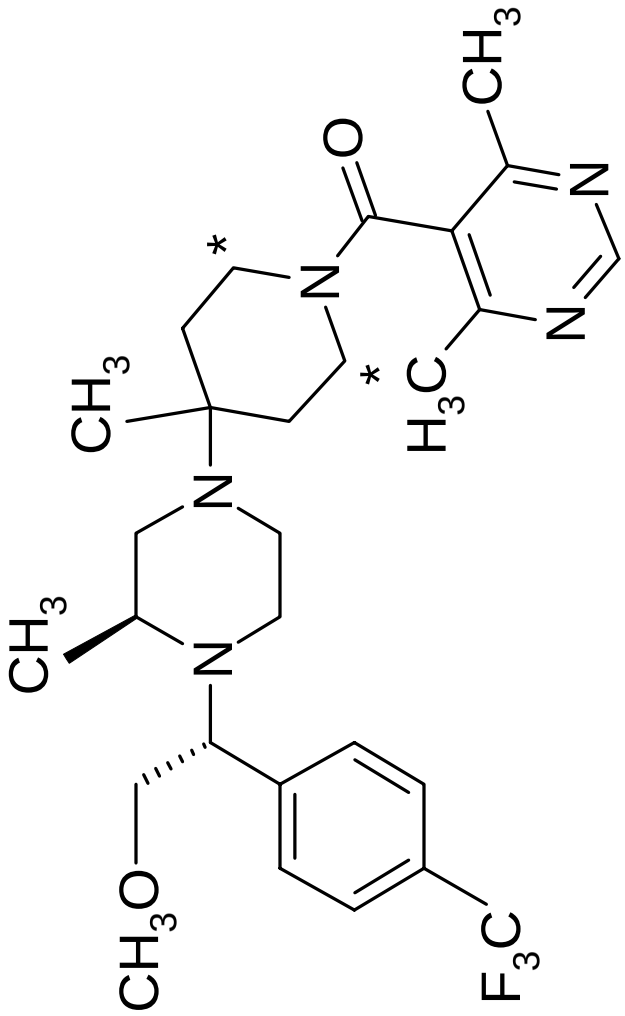


Fig. 1

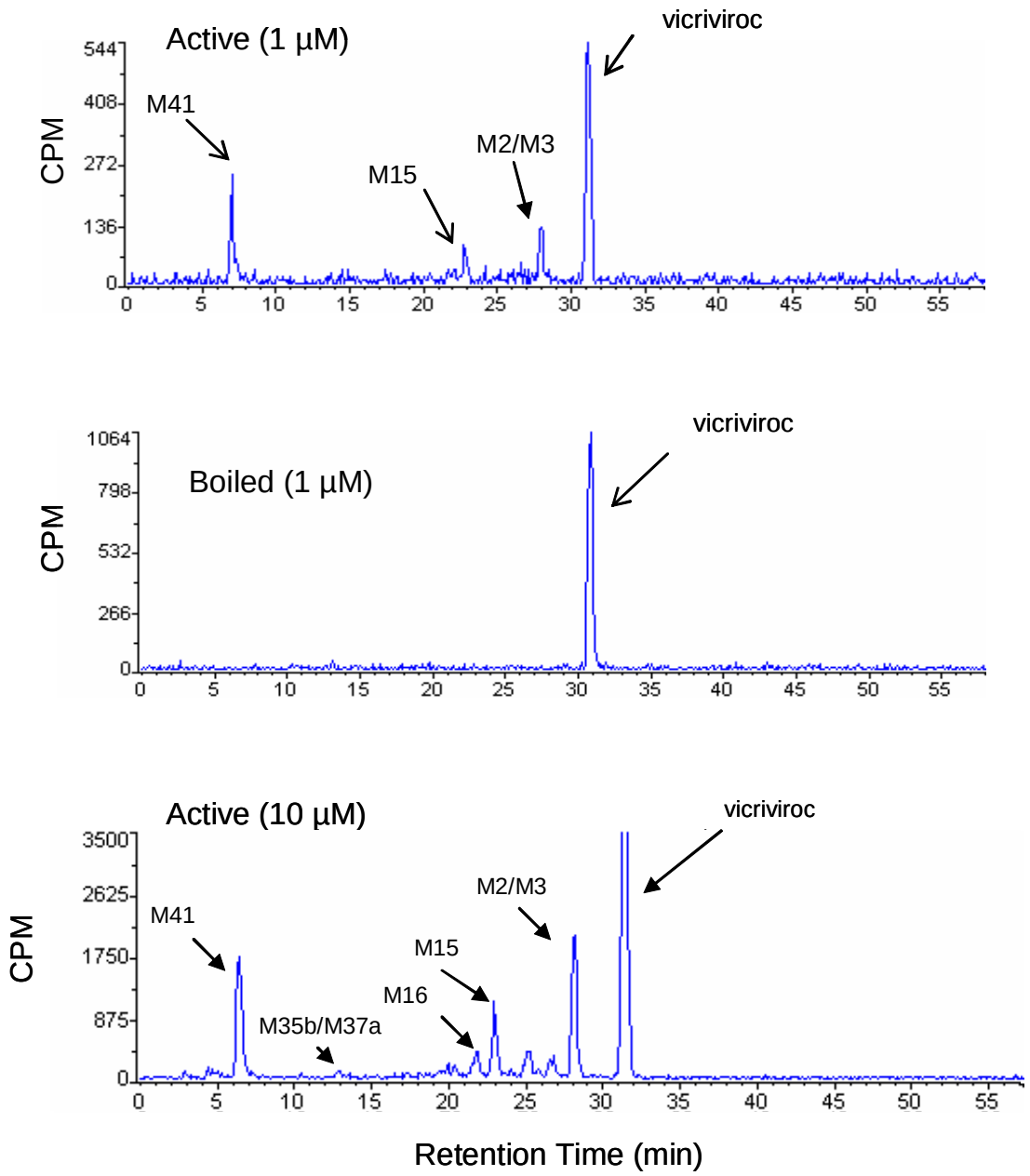


Fig. 2

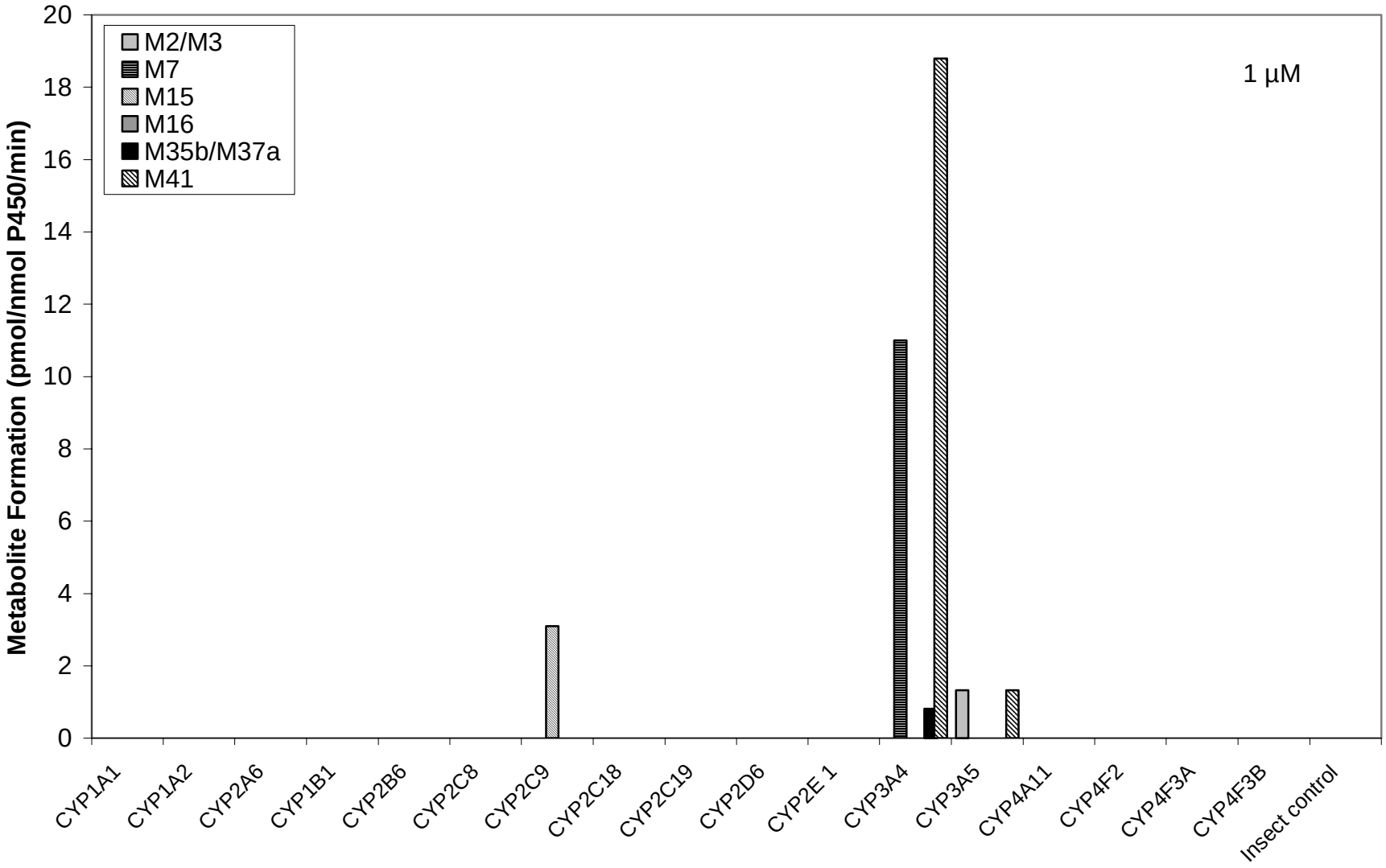


Fig. 3

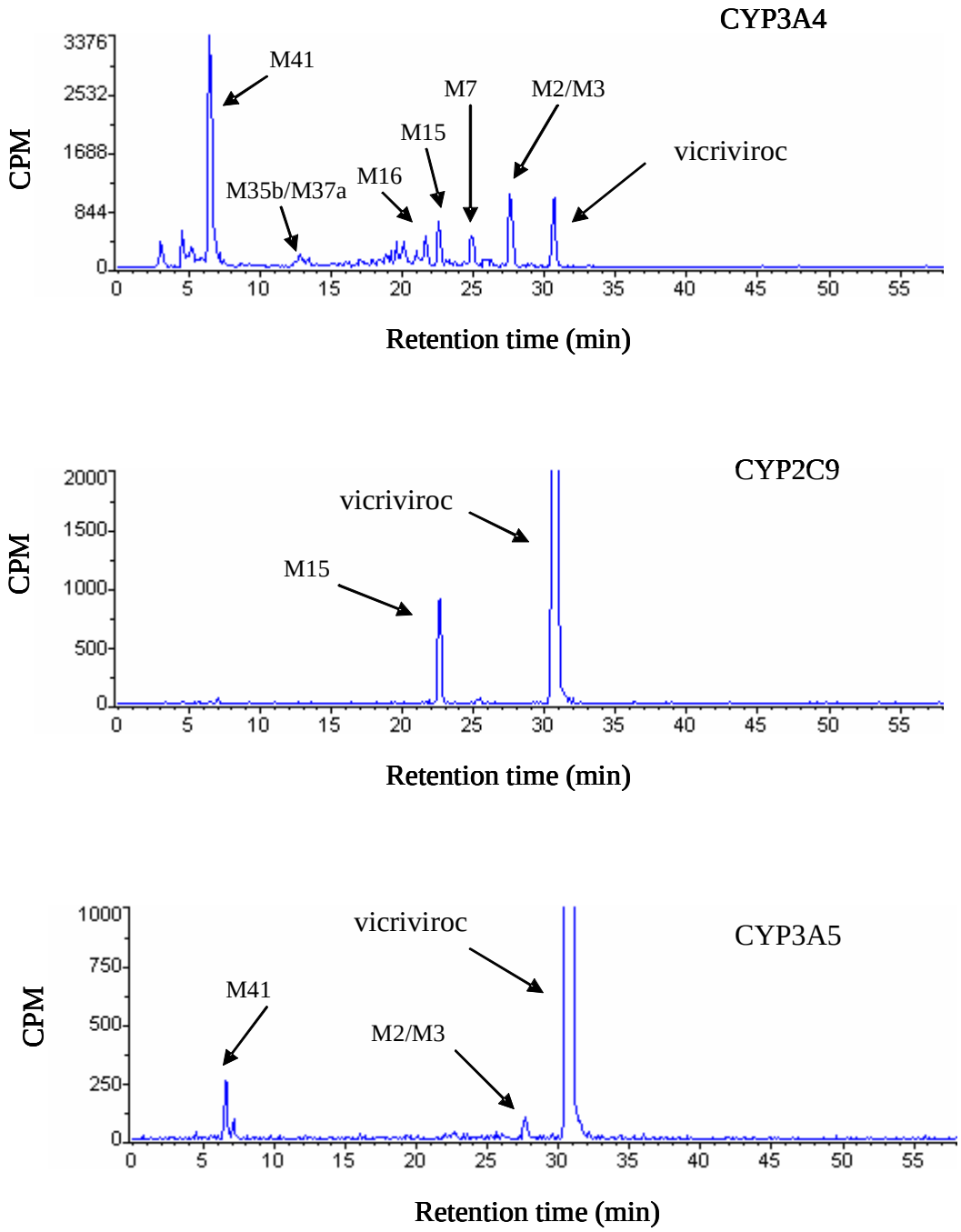


Fig. 4

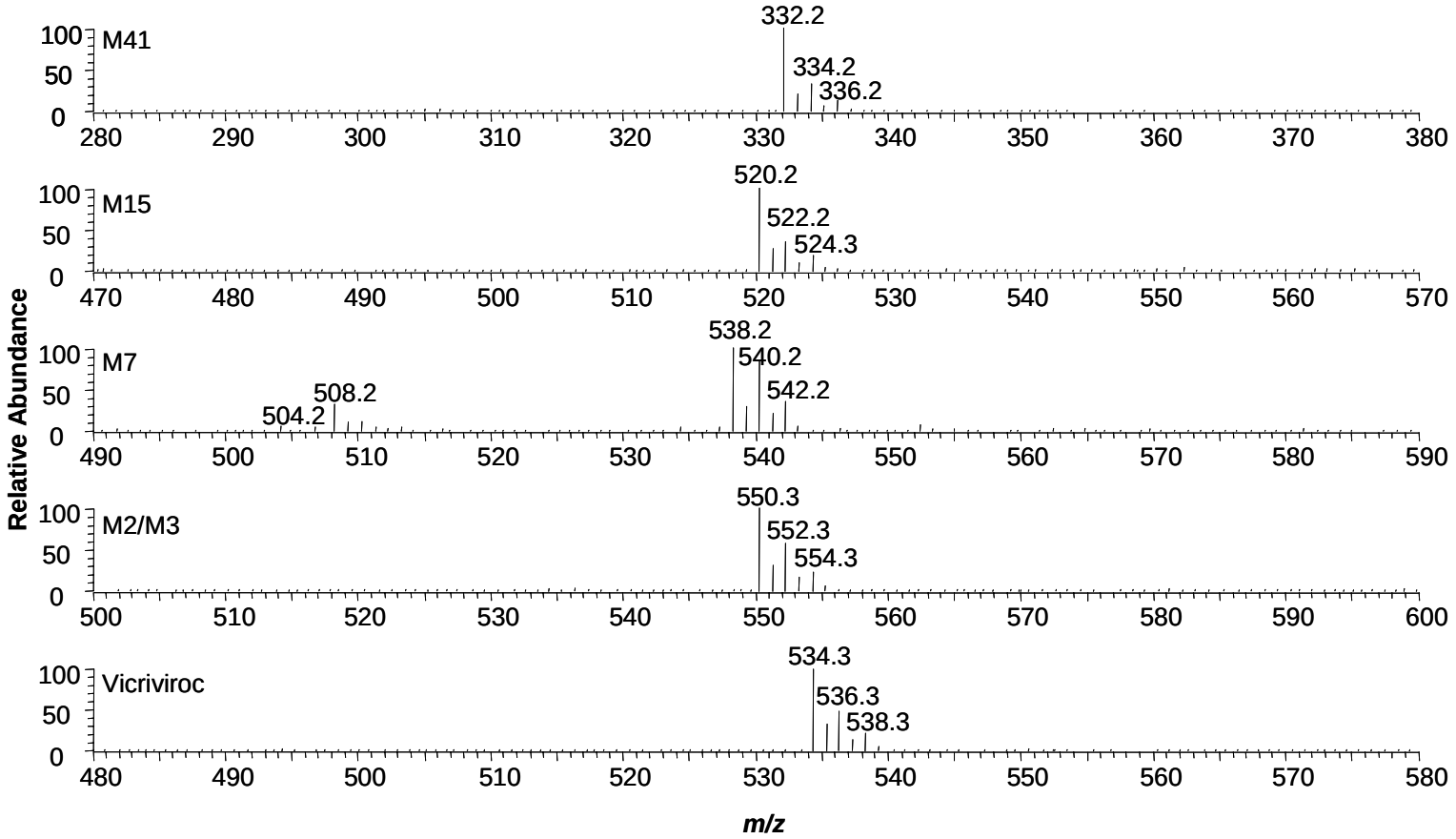


Fig. 5

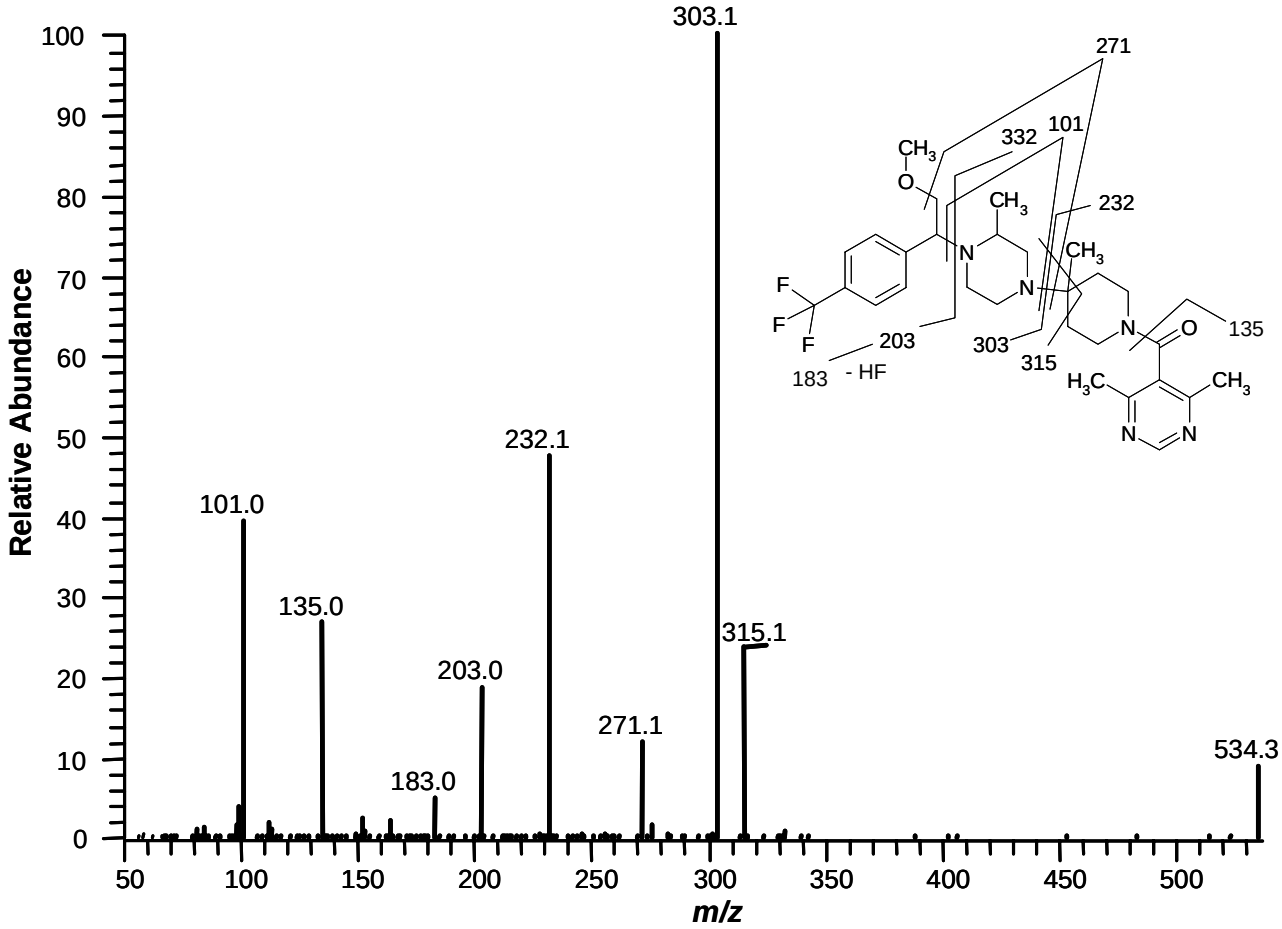


Fig. 6

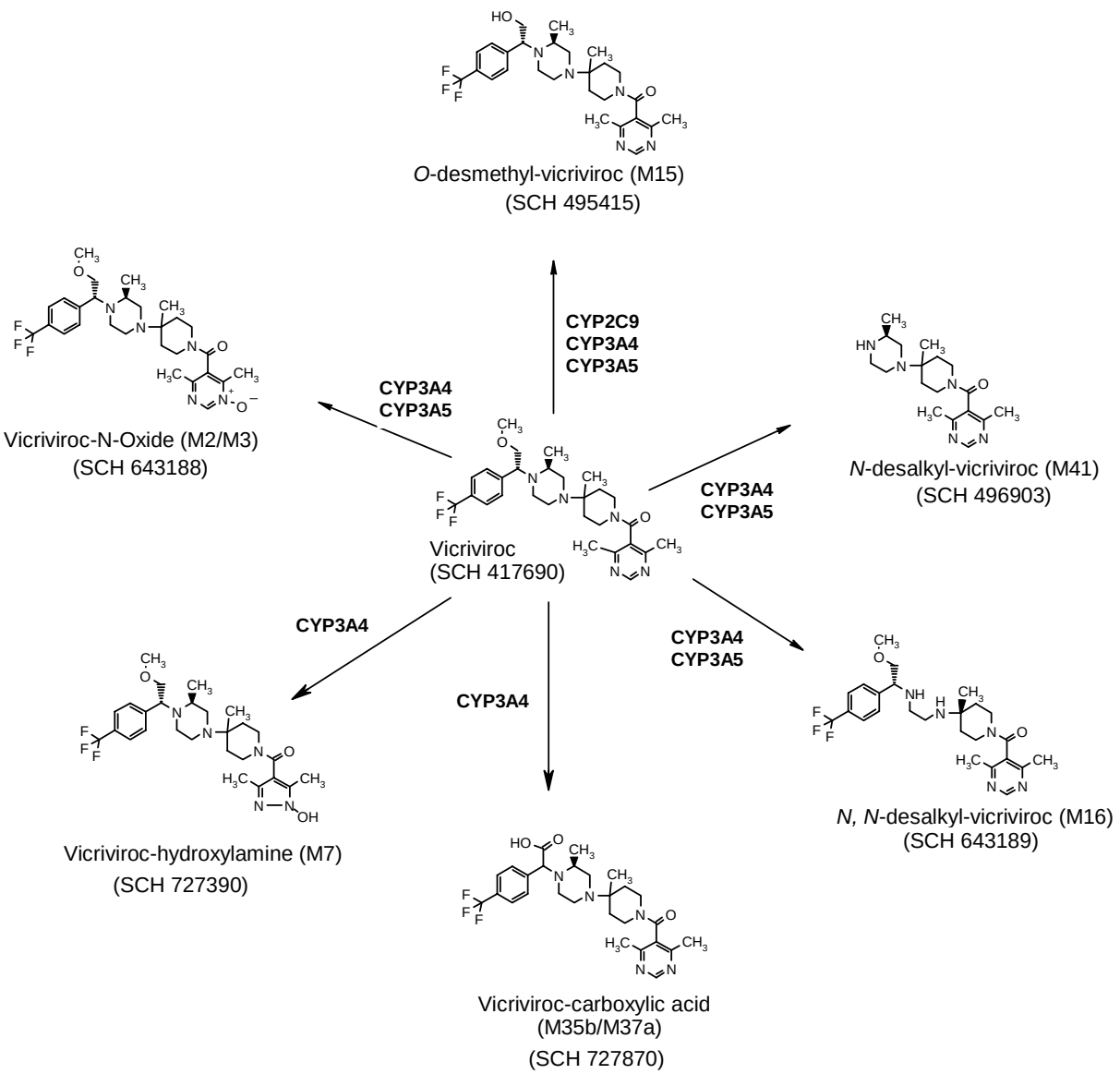


Fig. 7

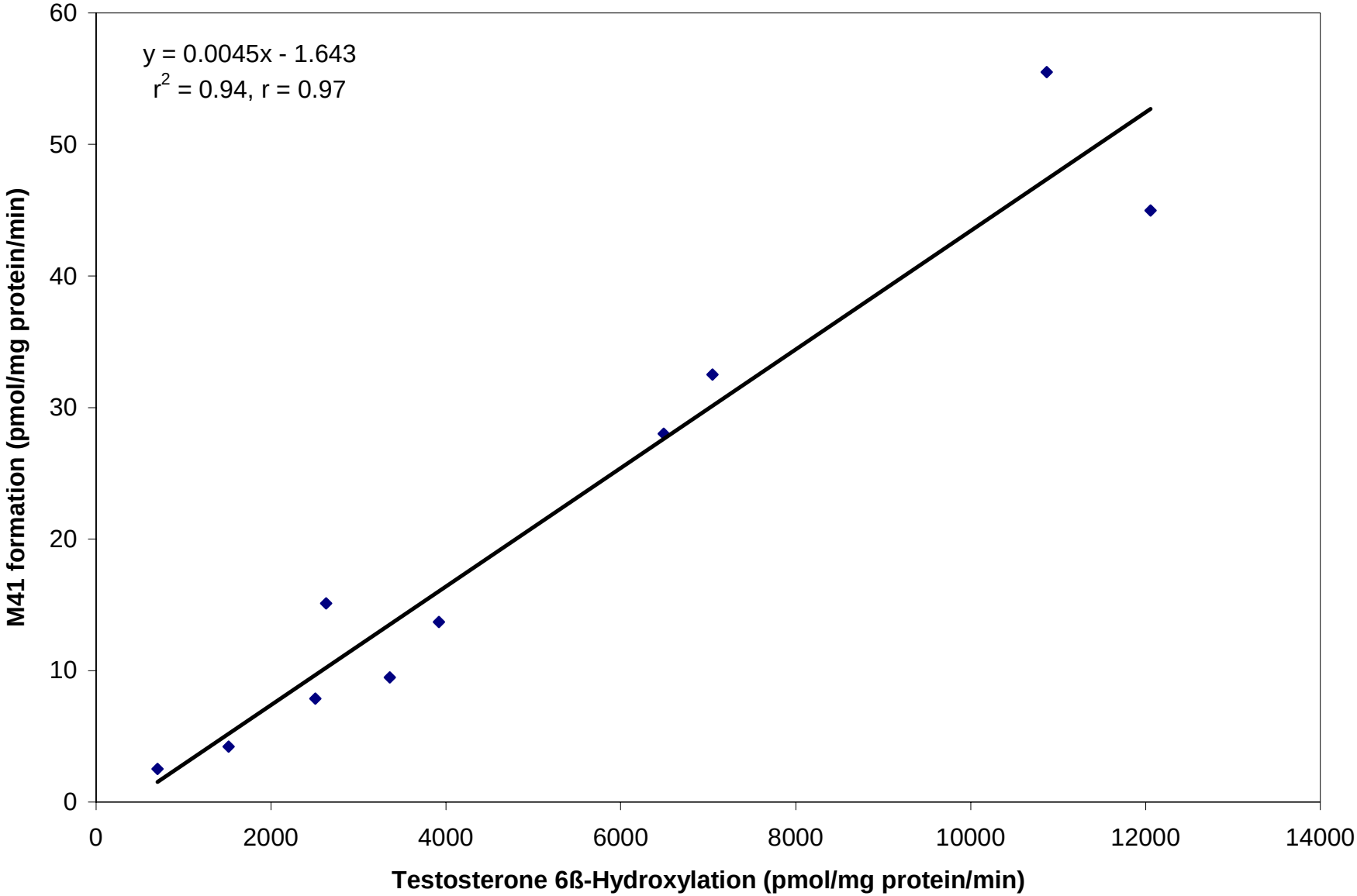


Fig. 8

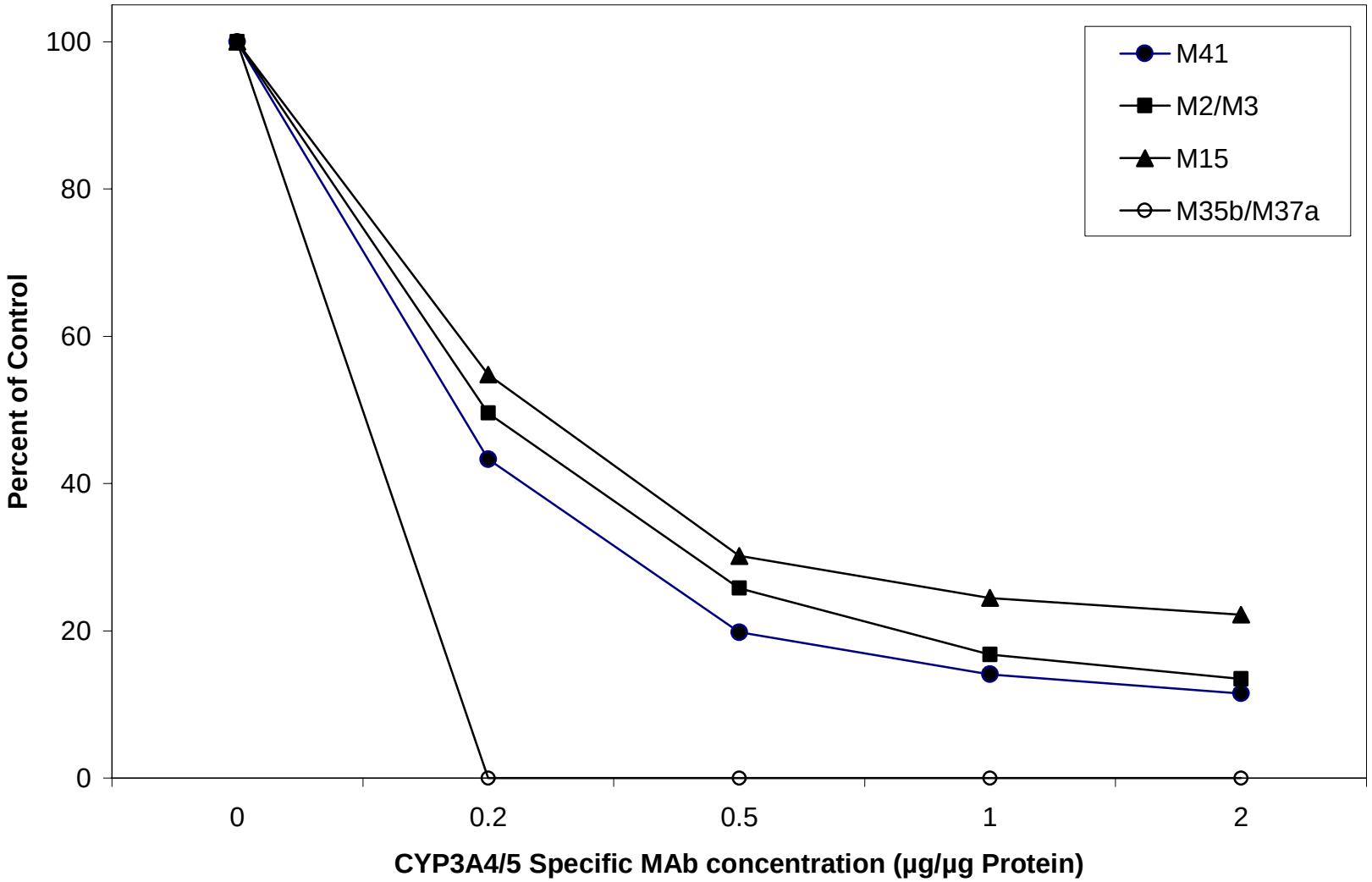


Fig. 9